Asian Journal of Electrical Sciences
ISSN: 2249-6297 (P) Vol.8, No.2, 2019, pp.42-49
© The Research Publication, www.trp.org.in
DOI: https://doi.org/10.51983/ajes-2019.8.2.2360

A Theoretical Study on the Thermoelectric Properties of Porous Armchair Germanene Nanoribbons

Varunpreet Kaur[1], Deep Kamal Kaur Randhawa[2] and Sukhdeep Kaur[3*]
[1&3]Department of Electronics Technology, Guru Nanak Dev University, Amritsar, Punjab, India
[2]Department of Electronics and Communication Engineering, Guru Nanak Dev University, RC Jalandhar, Punjab, India
[*]Corresponding author
E-Mail: kaurvarunpreet@gmail.com, randhawadk@gmail.com, gndusukhdeep@gmail.com

(Received 15 April 2019; Revised 2 May 2019; Accepted 22 May 2019; Available online 29 May 2019)

***Abstract* - Since the limits of conventional sources of energy are rapidly approaching, the thermoelectric devices have attracted attention for their potential of power generation directly from waste heat. In this paper, thermoelectric properties of porous armchair Germanene nanoribbons (AGeNRs) have been explored for a range of pore dimensions in order to achieve a high performance two-dimensional nanoscale thermoelectric device. The work has been done to investigate the influence of different nanopore shapes and their associated positions on the thermoelectric performance so as to tune it to the optimum pore shape and position that would enhance the overall thermoelectric efficiency. Also, the effect of passivation of the pore edges on thermoelectric parameters for all shapes has been studied. Further, the influence of temperature dependence on figure of merit has been observed. Ballistic transport regime and semi-empirical method using Huckel basis set is used to obtain the electrical properties while the Brenner potential is used for the phononic properties.**

***Keywords:* Thermoelectric, Nanoribbon, Figure of Merit, Nanopore, Thermal Conductivity.**

I. INTRODUCTION

The quest for a highly efficient thermoelectric device has attracted interest due to its significant potential in industrial applications. The ability of a device to convert a steady temperature gradient into an electrical current is given by efficiency of thermoelectric device, and was first discovered by Seebeck in 1821. The efficient performance of the thermoelectric device is characterized by a dimensionless parameter, called figure of merit $ZT=S^2GT/K$, where G is the electric conductance, S is the Seebeck coefficient, T is the temperature, and $K=K_e+K_{ph}$ is the total thermal conductivity that is summation of electron and phonon contributions respectively [1-3]. The electronic structure of germanene is similar to graphene and behaves like massless Dirac fermions [4]. However germanene has buckled structure which is responsible for better carrier mobility and stability as compared to graphene [5]. The high carrier mobility is due to the reason that carrier interactions of phonons in germanene are less than those of grapheme [6].

Several theoretical works have been carried for germanene nanoribbons (GeNRs). Since GeNR has a buckled structure like silicene, it can be expected that it is compatible with the silicon based electronic industry [7-8]. The researchers have investigated the thermal conductivity of graphene and silicene with respect to their length, temperature, width, and chirality [9-11]. Balatero [12] *et al.*, has studied about the thermal conductivity of germanene with respect to its length, temperature, width, and chirality. Further, the thermal, mechanical, optical, structural, magnetic and thermoelectronic properties of germanene in different ambient conditions have been investigated using first principle calculations and classical molecular dynamics [13-15]. Further, the investigation of the thermoelectric properties of silicon and germanium in one and two dimensional structures has been done using first-principles density functional techniques and also their linear response for the electrical and thermal transport has been studied. Different widths of the nanoribbons were considered for two-dimensional silicene and germanene, and they also investigated the possibility of nano structuring these systems by mixing silicon and germanium and it is found that the figure of merit of 2.5 at room temperature can be obtained [14]. Moreover, Hossain *et al.* reported the successful introduction of rectangular pores of different dimensions in the armchair graphene nanoribbons and was able to tune the pore to its optimal dimension which resulted in superior ZT approximately six times higher than pristine grapheme nanoribbon [16]. Inspiring by his work, porous GeNRs are studied by incorporating circular, triangular, rectangular and rhombus nanopores in this paper.

A dedicated research activity has been focused on nanostructured materials after the seminalwork by Hicks and Dresselhaus [17] for thermoelectric applications. Since our existing technology is based on semiconductors (germanium and silicon); it is therefore appears natural to look at the thermoelectric properties of these materials, since the integration of a thermoelectric device based on them would be simpler than the integration of carbon-based devices [5].

II. METHODOLOGY

In order to obtain the various parameters of thermoelectric property, the electron and phonon transmission are calculated using Extended Huckel Theory (EHT) and Non-Equilibrium Green's Function (NEFG) [18]. The bond length and buckling distance of germanene is taken as 2.46 Å and 0.73 Å respectively [19].

Within the Extended Huckel theory framework, $G^R = (ES_{ov}-H-\Sigma_L-\Sigma_R)^{-1}$ is the retarded Green function where $E$is the electron energy, H and S_{ov} are the Hamiltonian and overlap matrix of the central region respectively which are calculated from extended Huckel technique using Hoffman basis [20] and then solved using non-equilibrium Green function (NEFG) to yield the electron transmission function that can be obtained through relation:

$$T(E) = \mathrm{Trace}[\Gamma_R(E)\, G^R(E)\, \Gamma_L(E) G^{R\dagger}(E)] \quad (1)$$

where $\Gamma_{L,R}(E) = i(\Sigma_{L,R}(E) - \Sigma_{L,R\dagger}(E))$ describes the level broadening due to the coupling between the left / right electrodes and the central scattering region and $\Sigma_{L,R}(E)$ are the retarded self-energies for the electrodes. The mesh points in real space calculation are 1 × 1 × 100 k points, mesh cut-off at 10 Hartree and the temperature was set at 300K.

Once $T(E)$ is known, Seebeck Coefficient S, electrical conductance G and electronic thermal conductance K_e can be obtained under linear response approximation as [21]

$$G = \frac{I}{\Delta V}\Big|_{\Delta T = 0} = e^2 L_0 \quad (2)$$

$$S = -\frac{\Delta V}{\Delta T}\Big|_{I = 0} = \frac{L_1}{eTL_0} \quad (3)$$

$$k_e = \frac{I_Q}{\Delta T}\Big|_{IE = 0} = \frac{L_2 - L_1^2/L_0}{T} \quad (4)$$

where,

$$L_n = \frac{2}{h}\int dE\, T(E)\left(-\frac{\partial f}{\partial E}\right)(E-\mu)^n \quad (5)$$

Here L_n is Lorenz function, e is the charge of electron, h is the Planck constant, μ is the chemical potential, T is the average temperature and $\partial f/\partial E$ is the derivative [22] of the Fermi function ($f = 1 + \exp((E-\mu)/k_B T))^{-1}$)known as Fermi-Dirac distribution function.

To calculate the phonon thermal conductance, we used the Landauer approach [23]:

$$k_{ph} = \frac{h^2}{2\pi k_B T^2}\int d\omega\, \omega^2 T_{ph}(\omega)\left(\frac{\partial n}{\partial \omega}\right) \quad (6)$$

For phonon transmission $T_{ph}(\omega)$,$H$and S are substituted by a force constant matrix K, and a diagonal matrix of atomic mass M respectively. The term $\partial n/\partial \omega$ is the derivative of the Bose-Einstein distributionfor phonons. To calculate the force constant matrix for phonons, empirical Brener potential was used.

Both the electron and phonon transport simulations are performed in the Virtual NanoLab-Atomistix Toolkit (ATK) software package [24]. The electron-phonon interactions are neglected while carrying out independent electron and phonon calculations as done by Chen et al., for grapheme [25]. In this paper, the similar considerations are assumed for germanene nanoribbons also.

III. RESULTS AND DISCUSSION

Firstly, the thermoelectric performance of GeNRs embedded with different pore shapes with varying positions has been studied at temperature 300K. The length and width of the ribbon has been kept constant at 8.12 nm and 4.47 nm respectively. For pristine GeNR, the highest figure of merit obtained is 0.15. In later section, the effect of pore passivation and varying temperature on thermoelectric performance is also investigated.

A. Effect of Pore Shape and Position

In this section, the pore shapes, namely, circular, rectangular, triangular, rhombus with varying positions is studied. For each shape, different pore positions corresponding to center and respective edges (left and right) of nanoribbon has been evaluated. Further, the effect of increasing the nanopores from single to double has been predicted. The symmetry of the pores is maintained in every case.

1. Circular Pore

The atomistic model of our proposed armchair germanene nanoribbon structures with circular pores with varying pore positions is shown in Fig. 1. Each pore, as it clarifies, has its own associated edge terminations with two channels on both sides of the nanoribbon. The pore size is kept constant at a diameter of 1.7 nm. It is observed that in case of single pore, the position shows a no dependence on thermoelectric performance (ZT=0.3). While in double porous nanoribbon, the value of ZT increased to double (0.6). The variation in values of G, S, K and ZT are plotted w.r.t chemical potential (-2 to 2eV) for double porous structure as illustrated in Fig. 2. At the peak of ZT, the values of S and G are extracted as 208.4μV/K and 22.48μS respectively.

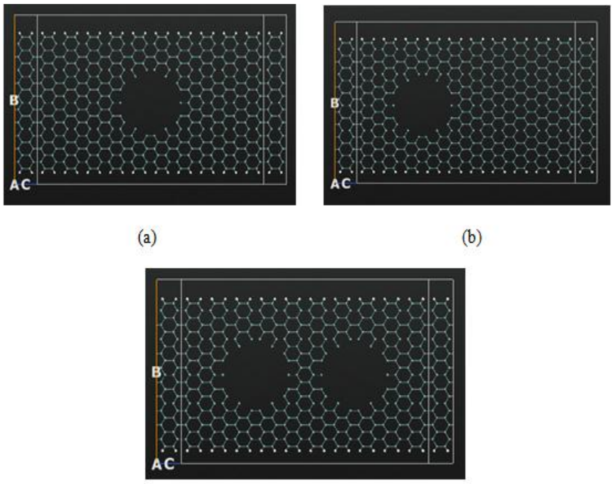

(a) (b)

(c)

Fig. 1 Geometrical optimized structure of the germanene nanoribbon with circular nanopore thermoelectric device with (a) single pore at center (b) single pore at left and (c) double pore

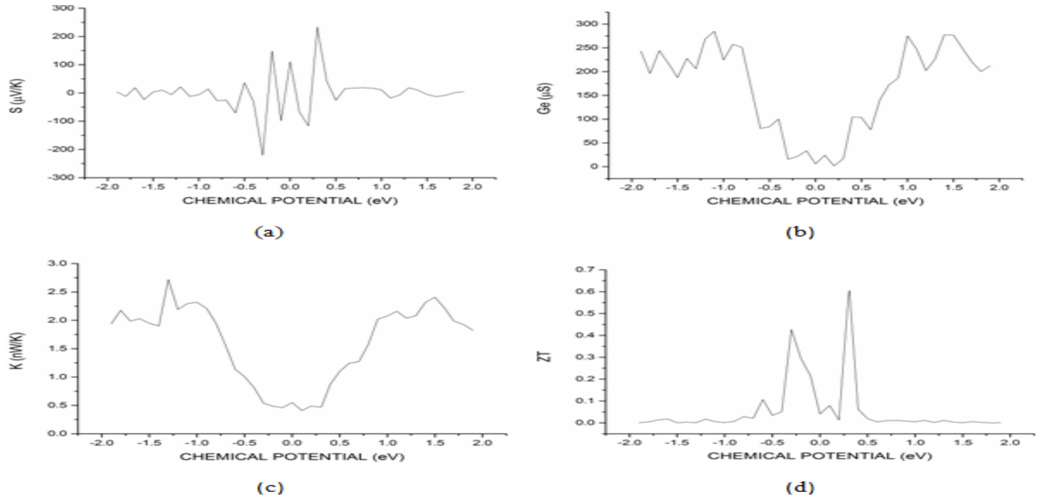

Fig. 2 (a) Seebeck coefficient (b) Electrical conductance (c) Thermal conductivity (d) Figure of merit for circular double porous nanoribbon

2. Triangular Pore

The armchair germanene nanoribbon embedded with triangular shaped pores is shown in Fig.3. The symmetrical orientation of the triangular pore embeds an equilateral triangle with each side of the triangle being 1.16h where h is the height of the triangle (in nm) such that the minimum number of atoms below and above the triangle corner edges should be same[18]. The height of the triangle is 1.82nm and therefore approximately side of triangle is taken as 2.13nm. It is analyzed that for single triangular pore (Fig. 3a-b), the peak of ZT rises to 0.24 while it gets approximately twice in double porous structure.

.

3. Rectangular Pore

The GeNRs incorporating rectangular pores with different pore positions is shown in Fig. 5. The length and width of the pore is kept constant as 2.46nm and 1.704nm respectively. In single porous structures (Fig. 5a and b), the highest value for ZT is remains same (0.15) at varying positions which signifies that there is no dependence of pore position on thermoelectric performance of germanene nanoribbons. While in double porous nanoribbon, the value of ZT increased to double (0.34). The dependence of G, S, K and ZT with respect to chemical potential is shown in Fig. 6.

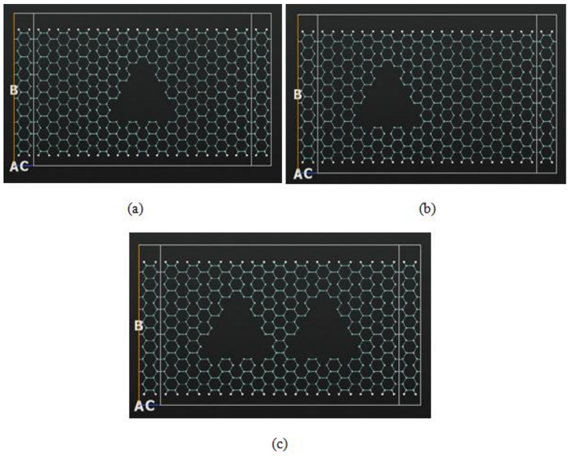

Fig. 3 Geometrical optimized structure of the germanenenanoribbon with triangular nanopore thermoelectric device with (a) single pore at center (b) single pore at left and (c) double pore

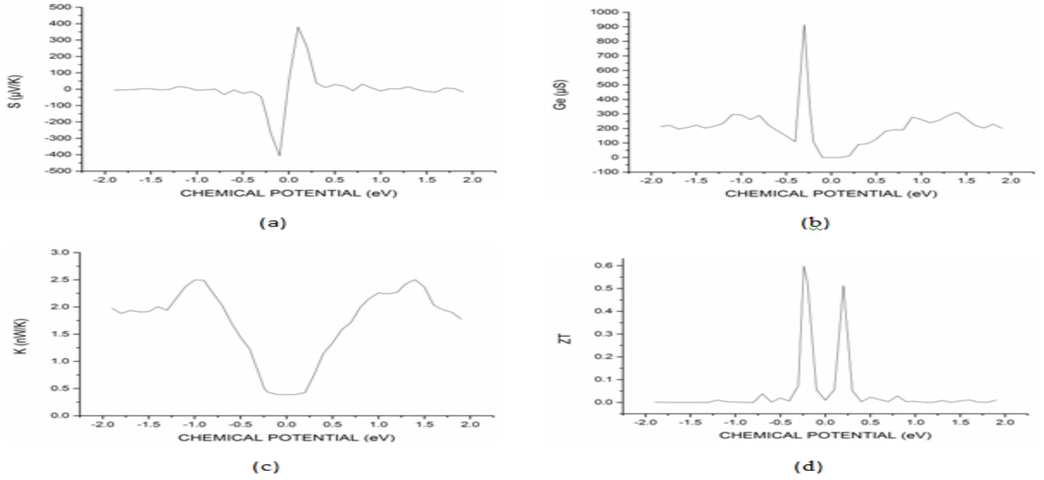

Fig. 4(a) Seebeck coefficient (b) Electrical conductance (c) Thermal conductivity (d) Figure of merit for triangular double porous nanoribbon

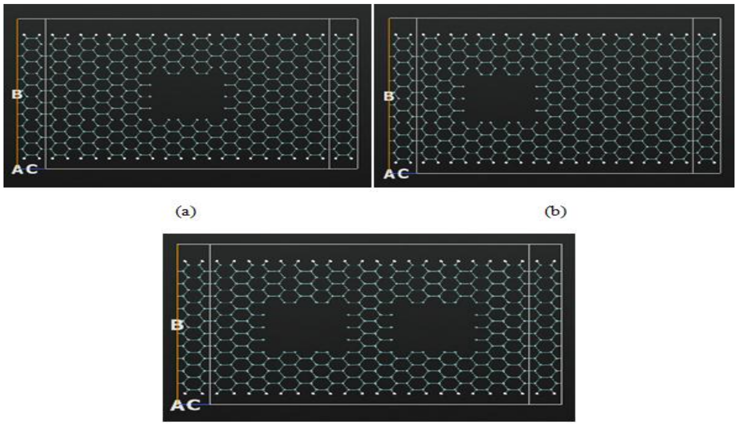

(a) (b)

(c)

Fig. 5 Geometrical optimized structure of the germanene nanoribbon with rectangular nanopore thermoelectric device with (a) single pore at center (b) single pore at left and (c) double pore

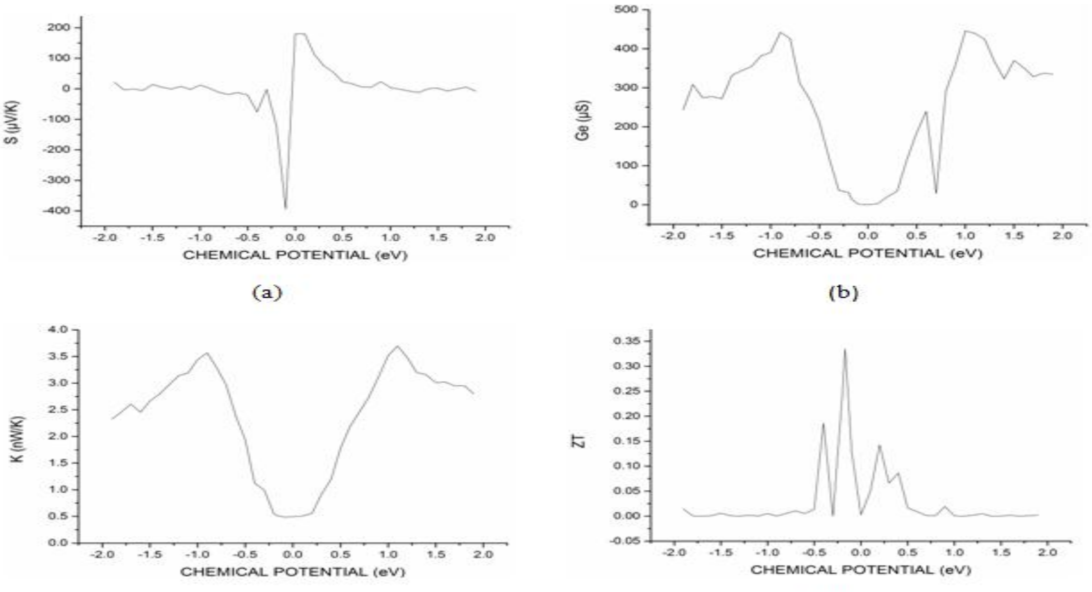

(a) (b)

(c) (d)

Fig. 6 (a) Seebeck coefficient (b) Electrical conductance (c) Thermal conductivity (d) Figure of merit for rectangular double porous structures

4. Rhombus Pore

The atomistic model of armchair germanene nanoribbon structures with rhombus pores with varying pore positions is shown in Fig. 7. The side of the rhombus is kept as 1.917nm in all three cases. It is observed that with single pore, the position shows a no dependence on thermoelectric performance (ZT=0.52). While in double porous nanoribbon, the value of ZT increased to 0.83.

Hereby also similar results are observed as in above three shapes i.e. double porous shows better figure of merit as compared to single porous structure. Further, the values of S, G, K, ZT are plotted with respect to chemical potential for double porous case. At peak of ZT, the values extracted for S and G are 230.2 μV/K and 23.32μS respectively.

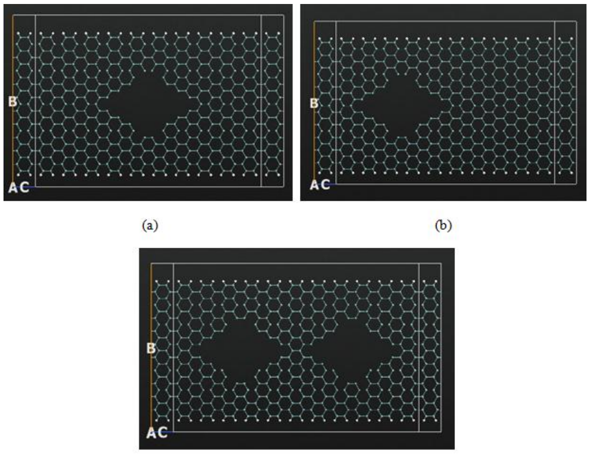

(a) (b)

(c)

Fig. 7 Geometrical optimized structure of the germanene nanoribbon with rhombus nanopore thermoelectric device with (a) single pore at center (b) single pore at left and (c) double pore

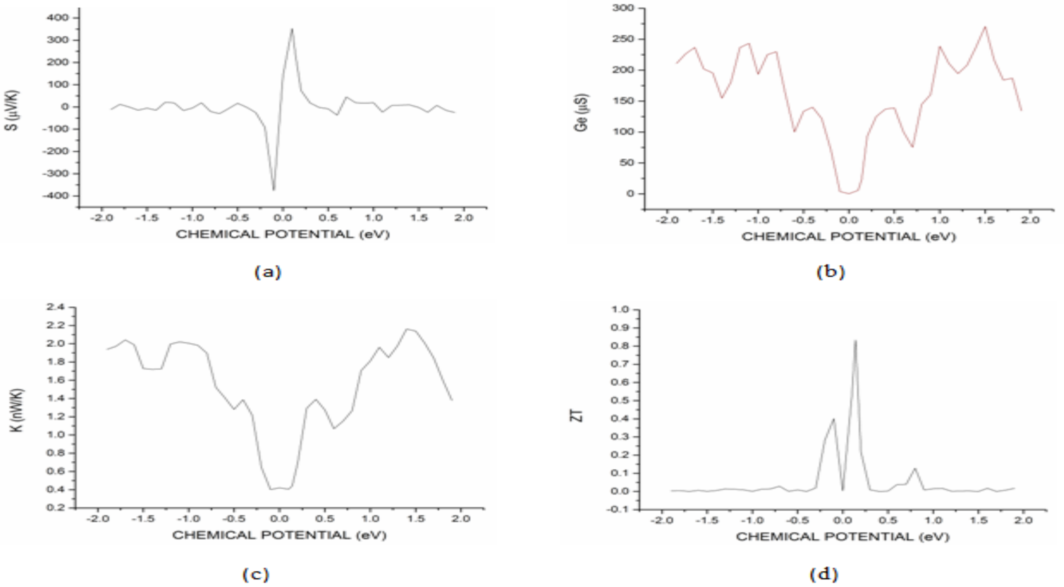

Fig. 8 (a) Seebeck coefficient (b) Electrical conductance (c) Thermal conductivity
(d) Figure of merit for rhombus double porous structures

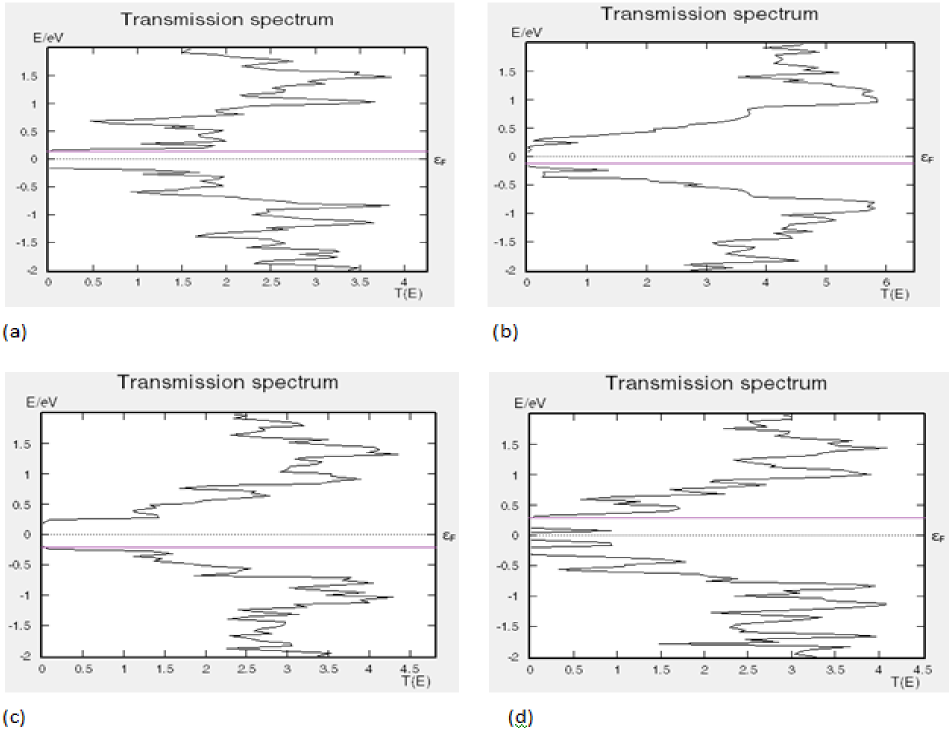

Fig. 9 Transmission spectrums for GeNR nanopore devices of (a) rhombus (b) rectangular (c) triangular (d) circular double porous structures with solid blue line representing the chemical potential at which peak ZT is observed. It is 0.14eV, -0.17eV, -0.24eV and 0.31eV respectively

5. Comparison of All Pore Shapes

To analyze the shape and position dependent thermoelectric properties, we compare the results obtained for all the pore shapes and their respective positions. Fig. 10 illustrates a comparative analysis among the peak ZT values evaluated for the different cases.

It is observed that rhombus nanopore structure shows the maximum figure of merit followed by circular pore, triangular shape and the rectangular being the last for single as well as double porous GeNRs. The subsequent order of ZT can be presented as

RHOMBUS>CIRCULAR>TRIANGULAR>
RECTANGULAR

It can be predicted from same figure that the position of the pore (left-center-right) has no dependence on the thermoelectric parameters. However, thermoelectric performance is enhanced with the addition of another pore as shown in the figure for a two pore structure.

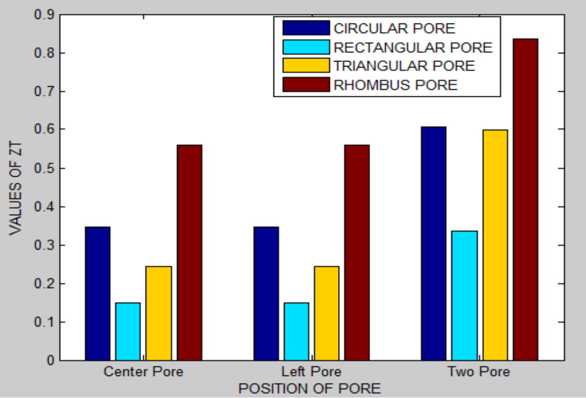

Fig. 10 Comparison of values of ZT of different nanopore shapes at different positions

B. Pore Passivation

The surface edges of the incorporated pores of above studied two porous structures are passivated with hydrogen to study their influence. Hydrogen has been chosen for passivation because of its ability to increase the structural stability [26].The results obtained for passivated pore edges are then compared with the non-passivated results obtained so far as demonstrated in Fig. 11(a-d).

As observed for Fig 12(a-d), the effects of pore passivation are not much pronounced for all shapes since there is no improvement on thermoelectric performance. The pore passivation results in corresponding decrease in values of G and S except for triangular pore where S is increased. Further, the values of K_{ph} shows increasing trend in all cases which can be due to the fact that the phonon-edge scattering becomes the dominant scattering mechanism suppressing the phonon-phonon scattering [27]. Overall, these parameters lead to the decrement of figure of merit. Thus, pore passivation is not suitable to improve thermoelectric performance of germanene nanoribbons.

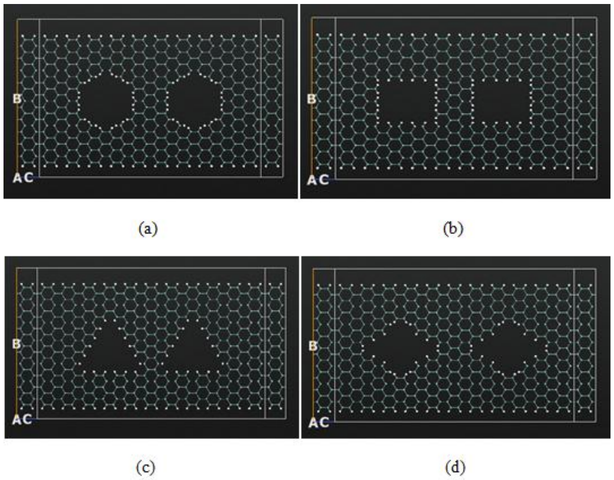

(a) (b)

(c) (d)

Fig. 11 Hydrogen passivated (a) Circular pore (b) rectangular pore (c) triangular pore (d) Rhombus pore

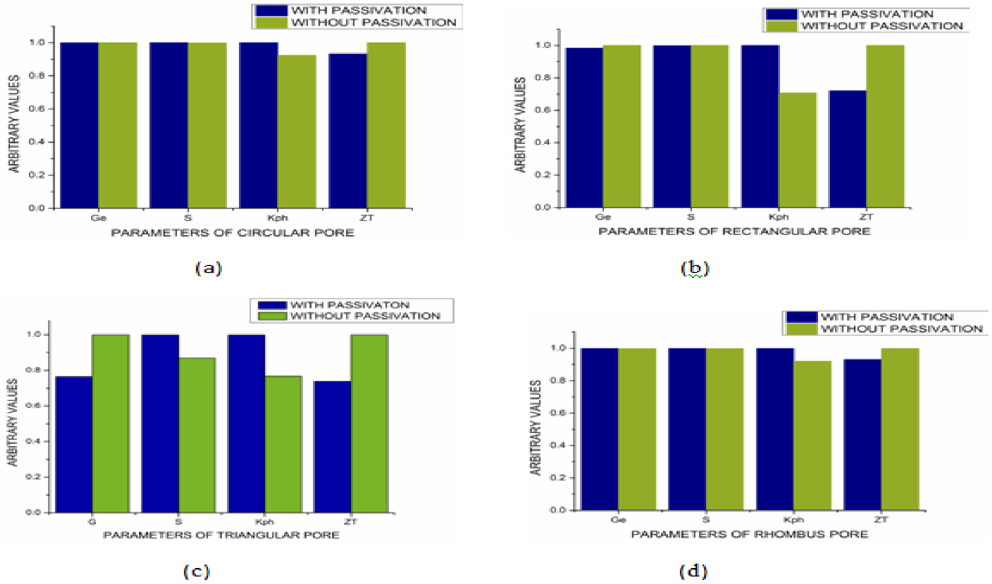

(a) (b)

(c) (d)

Fig. 12 Comparison ofvarious parameters of the passivated and non-passivated nanopores for (a) circular pore,(b) rectangular pore, (c) triangular pore, and (d) rhombus pore

C. Temperature Dependence

Fig. 13 illustrates the effect of varied temperature on thermoelectric performance of rhombus shaped single porous GeNRs. The response of thermoelectric devices with the variable temperature is observed because these devices usually operate in wide temperature range [18]. It is hereby observed that phonon as well as electrical thermal conductivity rises gradually with temperature as shown in Fig. 13(a). But owing to increase in power factor (S^2G) at low temperature levels of range 0-600K (Fig13.(b)) and the presence of temperature in numerator of ZT, figure of merit rises with increase in temperature from 0-600 K and then begins to decrease gradually (Fig13(c)). Thus, temperature affects ZT greatly. These calculations do not take into account the electron-phonon and electron-electron interactions which dominate at higher temperature.

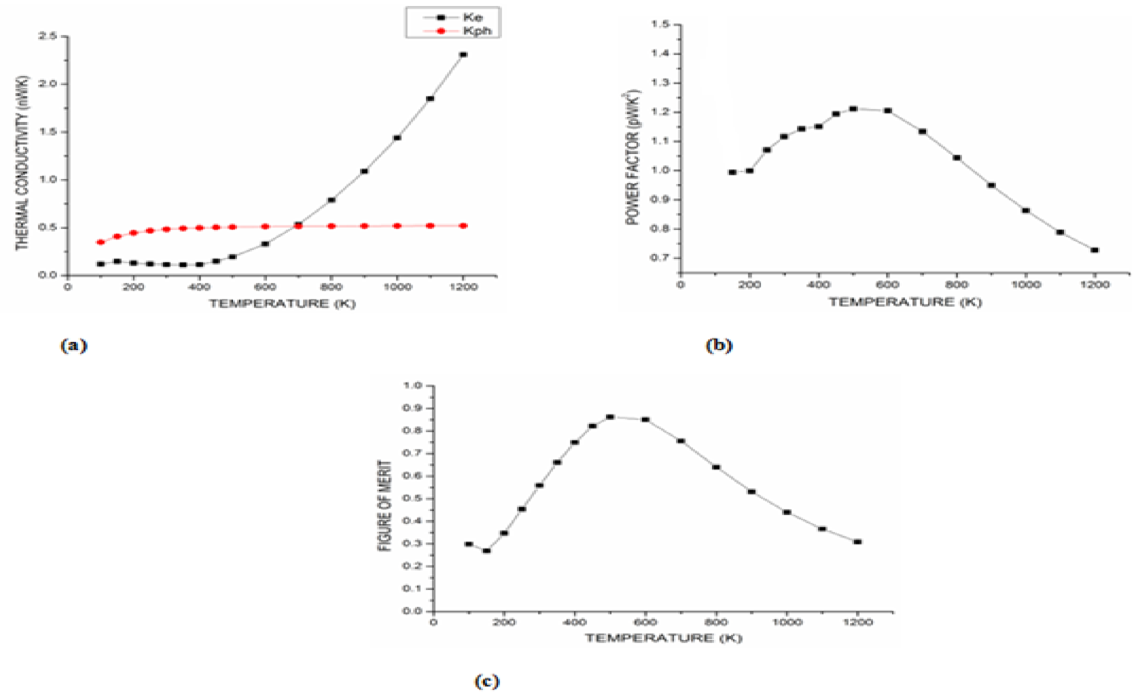

(a)

(b)

(c)

Fig. 13 Variation of (a) Thermal conductivity (b) Power factor
(c) Figure of merit with respect to temperature for rhombus single porous nanoribbon

IV. CONCLUSION

In summary, we have investigated the effect of different pore shape and its associated position on thermoelectric performance of of GeNRs nanopore devices. Nnaopores of different shapes i.e, circle, rectangle, triangle and rhombus have been introduced at varying positions of the nano-structure so as to study their influence on the thermoelectric figure of merit. By optimising the pore parameters, higher figure of merit is observed which is approximately 8 times higher than pristine GeNR. Further, influence of pore passivation is noted which results in decrement of ZT in all double porous shapes. In addition, the dependence of ZT of single pore GeNR on temperature is also studied and peak of ZT is observed at 600K. Thus, our work extends the idea towards achieving better thermoelectric devices by optimal pore engineering.

REFERENCES

[1] Daniel D. Pollock, Thermoelectricity; Theory, Thermometry, Tool, Philadelphia, ASTM Special Technical Publication 852, 1985.

[2] G.S. Nolas, J. Sharp, and H.J. Goldsmid, “Thermoelectrics: Basic principles and new materials developments”, *Springer series in Material Science.*, Berlin, Heidelberg: Springer, Vol. 45, 2001.

[3] H.J. Goldsmid, Ed.1, “Introduction to Thermoelectricity”, *Springer Series in Material Science*., Berlin: Springer, Vol. 121, pp. 250, 2010.

[4] H. Şahin, S. Cahangirov, M. Topsakal, E. Bekaroglu, E. Akturk, and R. T. Senger, “Monolayer honeycomb structures of group-IV elements and III-V binary compounds: First- principles calculations”, *Physical Review B.*, Vol. 80, pp. 155453, Oct. 2009.

[5] M. M. Monshi, S. M. Aghaei and I. Calizo, “Edge functionalized germanene nanoribbons: impact on electronic and magnetic properties”, *RCS advances*, Vol. 7, pp. 18900-18908, March 2017.

[6] N. J. Roome, and J. D. Carey, “Beyond graphene: stable elemental monolayers of silicene and germanene”, *ACS applied materials & interfaces*, Vol. 6, pp. 7743-7750, 2014.

[7] J. Yan, R. Stein, D.M. Schaefer, Xiao-Qian Wang, and M. Y. Chou, “Electron- Phonon Coupling in Two-Dimensional Silicene and Germanene”, *Physical Review B*., Vol. 88, 121403, August 2013.

[8] Z. Ni, Q. Liu, K. Tang, and J. Zheng *et al.*, “Tunable Bandgap in Silicene and Germanene”, *Nano Letters 2012*, Vol. 12, pp. 113–118, Nov. 2011.

[9] T. Y. Ng, J. Yeo, and Z. Liu, “Molecular dynamics simulation of the thermal conductivity of short strips of graphene and silicene: a comparative study”, *Int J Mech Mater Des.*, Vol. 9, No. 2, pp. 105-114, June 2013.

[10] Y. Wang, J. Zheng, and Z. Ni *et al.*, “Half-Metallic Silicene and Germanene Nanoribbons: towards High-Performance Spintronics Device”, *NANO: Brief reports and reviews*, Vol. 7, No. 5, pp. 1250037(1-9), April 2013.

[11] F. Bechstedt, L. Matthes, P. Gori and O. Pulci, “Infrared absorbance of silicone and germanene”, *Applied Physics Letter*., Vol. 100, 261906, June 2012.

[12] M.A. Balateroa, G. J. Paylagab, N. T. Paylagac, and R. V. Bantaculod, “Molecular Dynamics Simulations of Thermal Conductivity of Germanene Nanoribbons (GeNR) with Armchair and Zigzag Chirality”, *Applied Mechanics and Materials*, Vol. 772, pp. 67-71, April 2015.

[13] G. Baskaran, *Room Temperature Superconductivity, Spin Liquid and Mott Insulator: Silicene and Germanene as prospective playgrounds*, September, 2013.

[14] K. Yang, S. Cahangirov, A. Cantarero, A. Rubio, and R. D'Agosta, “Thermoelectric properties of atomic-thin silicene and germanene nano-structures”, *Physical Review B.*, Vol. 89, pp. 125403, October 2013.

[15] M. Houssaa, B. Broeka, E. Scalisea, G. Pourtoisb, V.V Afanas'eva, and A. Stesmansa, “Theoretical Study of Silicene and Germanene”, *ECS Transactions*., Vol. 53, No. 1, pp. 51-62, May 2013.

[16] M.S. Hossain, F.A. Dirini, F.M. Hossain, and E. Skafidas: “High-performance graphene nano-ribbon thermoelectric devices by incorporation and dimensional tuning of nanopores”, *Sci. Rep*., Vol. 5, 11297, June 2015.

[17] L. D. Hicks, and M. S. Dresselhaus, “Effect of quantum-well structures on the thermoelectric figure of merit”, *Phys. Rev. B.*, Vol. 47, pp. 12727, May 1993.

[18] S. Kaur, S. B. Narang and D. K. Randhawa, “Influence of the pore shape and dimension on the enhancement of thermoelectric

performance of graphene nanoribbons", *Journal of Materials Research*., Vol. 32, pp. 1149-1159, Dec. 2016.

[19] S.M. Aghaei, M.M. Monshi, I. Torres, M. Banakermani, and I. Calizo, "Lithium-functionalized germanene: A promising media for CO_2 capture", *Physics Letters A*., Vol. 382, pp. 334-338, Feb. 2018.

[20] D. Kienle, J.I. Cerda, and A.W. Ghosh, "Extended Huckel Theory for band structure, chemistry, and transportI. Carbon nanotubes", *Journal of Applied Physics*, Vol. 100, 043714, August 2006.

[21] M.S. Hossain, F. Al-Dirini, F.M. Hossain, and E. Skafidas, "High performance graphenenano-ribbon thermoelectric devices by incorporation and dimensional tuning of nanopores", *Sci. Rep*., Vol. 5, 11297, June 2015.

[22] K. Esfarjani, M. Zebarjadi, and Y. Kawazoe, "Thermoelectric properties of a nanocontact made of two-capped single-wall carbon nanotubes calculated within the tight-binding approximation", *Phys. Rev. B*: *Condens. Matter Mater. Phys.,* Vol. 73, pp. 403-406, Feb.2006.

[23] R. Landauer, "Spatial variation of currents and fields due to localized scatterers in metallic conduction", *IBM. J. Res. Dev.*, Vol. 1, pp. 223, July 1957.

[24] K. Stokbro, D.E. Petersen, S. Smidstrup, A. Blom, M. Ipsen, and K. Kaasbjerg, "Semiemperical model for nanoscale device simulations", *Phys. Rev. B:Condens. Matter Mater. Phys.*, Vol. 82, 075420, August 2010.

[25] J.H. Chen, C. Jang, S. Xiao, M. Ishigami, and M.S. Fuhrer, "Intrinsic and extrinsic performance limits of graphene devices on SiO_2", *Nat. Nano*., Vol. 3, pp. 206-209, April 2008.

[26] L. Pan, H.J. Liu, X.J. Tan, H.Y. Lv, J. Shi, X.F. Tang, and G. Zheng, "Thermoelectric properties of armchair and zigzag silicone nanoribbons", *Physical Chemistry Chemical Physics*, Vol. 14, pp. 13588– 13593, July 2012.

[27] L.Hu, and D. Maroudas, "Thermal transport properties of grapheme nanomeshes", *Journal of Applied Physics*, Vol. 116, 184304, Oct. 2014.